Recovery From Monocular Deprivation Using Binocular Deprivation

Brian S. Blais, Mikhail Y. Frenkel, Scott R. Kuindersma, Rahmat Muhammad, Harel Z. Shouval, Leon N Cooper and Mark F. Bear

J Neurophysiol 100:2217-2224, 2008. First published 23 July 2008; doi:10.1152/jn.90411.2008

Journal of Neurophysiology publishes original articles on the function of the nervous system. It is published 12 times a year (monthly) by the American Physiological Society, 9650 Rockville Pike, Bethesda MD 20814-3991. ISSN: 0022-3077, ESSN: 1522-1598. Visit our website at http://www.the-aps.org/.

J Neurophysiol 100: 2217–2224, 2008.
First published July 23, 2008; doi:10.1152/jn.90411.2008.

Recovery From Monocular Deprivation Using Binocular Deprivation

Brian S. Blais,[1,2] Mikhail Y. Frenkel,[3] Scott R. Kuindersma,[6] Rahmat Muhammad,[3] Harel Z. Shouval,[2,4] Leon N Cooper,[2,5] and Mark F. Bear[3]

[1]*Department of Science and Technology, Bryant University, Smithfield, Rhode Island;* [2]*Institute for Brain and Neural Systems, Brown University, Providence, Rhode Island;* [3]*Howard Hughes Medical Institute, The Picower Institute for Learning and Memory, Department of Brain and Cognitive Sciences, Massachusetts Institute of Technology, Cambridge, Massachusetts;* [4]*Department of Neurobiology and Anatomy, University of Texas Medical School at Houston, Houston, Texas; and* [5]*Department of Physics, Brown University, Providence, Rhode Island; and* [6]*Department of Computer Science, University of Massachusetts, Amherst, Massachusetts*

Submitted 27 March 2008; accepted in final form 17 July 2008

Blais B, Frenkel M, Kuindersma S, Muhammad R, Shouval HZ, Cooper LN, Bear MF. Recovery from monocular deprivation using binocular deprivation. *J Neurophysiol* 100: 2217–2224, 2008. First published July 23, 2008; doi:10.1152/jn.90411.2008. Ocular dominance (OD) plasticity is a robust paradigm for examining the functional consequences of synaptic plasticity. Previous experimental and theoretical results have shown that OD plasticity can be accounted for by known synaptic plasticity mechanisms, using the assumption that deprivation by lid suture eliminates spatial structure in the deprived channel. Here we show that in the mouse, recovery from monocular lid suture can be obtained by subsequent binocular lid suture but not by dark rearing. This poses a significant challenge to previous theoretical results. We therefore performed simulations with a natural input environment appropriate for mouse visual cortex. In contrast to previous work, we assume that lid suture causes degradation but not elimination of spatial structure, whereas dark rearing produces elimination of spatial structure. We present experimental evidence that supports this assumption, measuring responses through sutured lids in the mouse. The change in assumptions about the input environment is sufficient to account for new experimental observations, while still accounting for previous experimental results.

INTRODUCTION

Ocular dominance (OD) plasticity in visual cortex is a powerful paradigm to study how experience and deprivation modify connections in the brain. In the classic experiments of Wiesel and Hubel, a rapid ocular dominance shift was achieved through the occlusion of one eye (Law et al. 1994; Wiesel and Hubel 1963). Monocular lid suture (MS) causes cortical neurons to lose responsiveness to the deprived eye by a process that is dependent on the structure of activity in the deprived eye (Blakemore 1976; Rittenhouse et al. 1999, 2006) and not simply on the decrease in light intensity. Various deprivation experiments that were traditionally performed in cats and have recently been replicated in rodents (Frenkel and Bear 2004; Mrsic-Flogel et al. 2007; Sawtell et al. 2003). Among other advantages, rodent visual cortex is amenable to chronic monitoring of the changes caused by deprivation. The results have challenged existing notions about the mechanisms responsible for deprivation.

We have previously shown that the Bienenstock, Cooper and Munro (BCM) (Bienenstock et al. 1982) learning rule, implemented in simulations with patterned environments composed of natural images, can account for normal rearing and various deprivation experiments (Blais et al. 1999; Law et al. 1994). Modeling studies of ocular dominance plasticity were based on the assumption that inputs to the cortex from the deprived channel are active, but lack a spatial structure (i.e., correlations). We have even been able to account for the difference between deprivation using MS and deprivation caused by a TTX injection into the eye [monocular inactivation (MI)] (Frenkel and Bear 2004; Rittenhouse et al. 1999) simply by assuming that the activity in these different forms of deprivation has a different variance (Blais et al. 1999). Here we present experimental results in which a period of monocular deprivation is followed by either binocular lid suture (BS) or by placing the animals in the dark (DE). These two different variants produce significantly different experimental outcomes; a difference that cannot be explained by our previous assumptions.

To account for deprivation results in mouse, we developed an input environment derived from natural images, with parameters appropriate for the mouse visual system. We altered our assumption about the impact of visual deprivation and assumed that the input through a sutured eye preserves a degraded version of the structured, patterned, input, an assumption consistent with previous experimental results in ferret (Krug et al. 2001), and with new experimental results presented here. With these new assumptions, we can account for the surprising and new experimental results regarding the difference between BS and DE while still being able to account for previous experiments.

METHODS

Animal surgery and visually evoked potential recording

Animal surgery, visually evoked potential (VEP) recordings, and visual stimulation protocols were performed as previously described (Frenkel and Bear 2004; Frenkel et al. 2006; Sawtell et al. 2003). Briefly, a head post was attached to the skull and a recording electrode was implanted into layer 4 of the binocular zone of either the right or left primary visual cortex in mice at postnatal day 25 (P25). After $\geq$24–48 h of recovery, mice were habituated to a head restraint apparatus. Animals were placed in front of a computer monitor occupying their binocular visual field. VEPs in response to sinusoidal gratings of low spatial frequency (0.05 cycles/deg) square-reversing at 1 Hz were recorded on P28. Both contralateral and ipsilateral eye responses were collected. Subsequently the visual environment was altered for 3–7 days by performing one of the following procedures:

Address for reprint requests and other correspondence: M. F. Bear, Picower Inst. for Learning and Memory, Massachusetts Inst. of Technology, 77 Massachusetts Ave., 46-3301, Cambridge, MA 02139 (E-mail: mbear@mit.edu).

The costs of publication of this article were defrayed in part by the payment of page charges. The article must therefore be hereby marked "*advertisement*" in accordance with 18 U.S.C. Section 1734 solely to indicate this fact.

monocular lid suture (MS), binocular lid suture (BS), monocular inactivation (MI) by intraocular TTX injections, or putting the animals into a light-tight room (DE). After 3–7 days, VEPs were recorded again in response to stimulation of contra- and ipsilateral eyes. In experiments to determine the effect of binocular lid closure on VEPs, baseline recordings were obtained with the eyes open using the spatial frequency that we determined to be optimal, namely 0.05 cycles/degree, The animals were anesthetized and the eyelids sutured. Following recovery from anesthesia, the VEPs were recorded again in response to the same stimuli with the eyes closed. At the end of all experiments, the animals were killed, and the brains were processed for electrode placement verification. All animal procedures were done in accordance with the guidelines of MIT Animal Care and Use Committee.

Simulation training patterns

To approximate the mouse visual system, we start with the following basic properties of the retina, lateral geniculate nucleus (LGN), and cortex. There are ~1,000 photoreceptors feeding into one ganglion cell (Jeon et al. 1998; Sterling et al. 1988), and there is not much difference in cell density for mouse or cat retina. In both cat and mouse, the retina/LGN responses show a center-surround organization, but with a center diameter around 7–10° for the mouse and <1° for cat (Grubb and Thompson 2003; Stone and Pinto 1993). Unlike the cat, the mouse has a functional contralateral bias on the order of ~2.5–1 (Drager and Olsen 1980; Frenkel and Bear 2004; Sawtell et al. 2003).

We use natural scene stimuli for the simulated inputs to the visual system. We start with images taken with a digital camera, with dimensions of 1,200 by 1,600 pixels and 40 by 60° real-world angular dimensions (Fig. 1*A*). We model the ganglion responses using a 32 × 32 pixel center-surround difference-of-Gaussians (DOG) filter to process the images, each pixel representing one photoreceptor. The center-surround radius ratio used for the ganglion cell is 1:3, with balanced excitatory and inhibitory regions and normalized Gaussian profiles. To correspond to the experimentally determined retinal properties, the images are rescaled before the DOG filter so that the center pixel size of the filter corresponds the real-world center size of 7° for the mouse. The original images are reduced to make each pixel correspond to their proper real-space size, and the ganglion response filter is applied. We include rotated versions of these filtered images to make the environment more symmetric and to eliminate any possible biasing effect of small numbers of patterns. The result is 3,000 images, each of which has a size of 26 × 26 pixels. These images represent the ganglion cell responses during natural viewing. Figure 1*A* shows the original images, and the processed images that represent ganglion cell responses are shown in Fig. 1*B*.

The specific biological details of the origin of the contralateral bias are not well known. To simply model the contralateral bias, we assume that the measured responses ($r_{\text{contra-lateral}}$) are the combined responses of two populations of cells: purely binocular and purely monocular cells (Fig. 1*C*). Thus the contralateral responses arise as a mixture of both monocular and binocular cell responses, and the ipsilateral responses reflect binocular responses only

$$r_{\text{contra-lateral}} = y_{\text{binocular-contra}} + y_{\text{monocular}}$$

$$r_{\text{ipsi-lateral}} = y_{\text{binocular-ipsi}}$$

where $y_{\text{binocular-contra}}$ is the response of binocular cells stimulated through the contralateral channel only, and $y_{\text{binocular-ipsi}}$ is the response of binocular cells stimulated through the ipsilateral channel only.

We assume that normally developed binocular cells have equal response to contra- versus ipsilateral stimulation ($y_{\text{binocular-contra}} \approx y_{\text{binocular-ipsi}}$), and further, that under these circumstances, the monocular and binocular cells contribute equally to the contralateral responses ($y_{\text{binocular-contra}} \approx y_{\text{monocular}}$). Thus under normal conditions, the contralateral response will be approximately twice the ipsilateral response, giving rise to the roughly 2 to 1 ratio of contra- to ipsilateral responses (C/I ratio) observed experimentally.

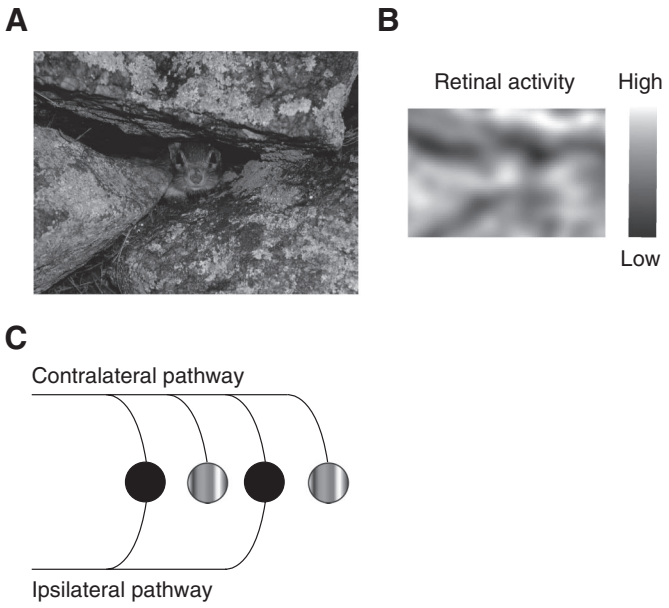

FIG. 1. Model assumptions, natural images, and contralateral bias. Inputs that drive receptive field development as derived from natural images. *A*: an example of an original image. *B*: the resulting distribution of retinal ganglion cell and lateral geniculate nucleus (LGN) neuron activity, using parameters appropriate for modeling the mouse visual system. The filter used is a difference-of-Gaussians (DOG) with a center/surround radius ratio of 1–3. *C*: the rodent visual system has a strong contralateral bias. We use a simplified architecture to model the contralateral bias. Two pools of cells combine to give responses. Binocular cells (black) respond equally to contra and ipsilateral stimulation, whereas monocular cells (gray) respond only to contralateral stimulation. If the number of binocular cells is equal to the number of monocular cells, then the contra-to-ipsilateral response ratio (C/I) will be ~2:1.

Synaptic modification

We use a single neuron and the parabolic form of the BCM (Bienenstock et al. 1982) learning rule for all of the simulations, where the synaptic modification depends on the postsynaptic activity, y, in the following way for a single neuron

$$\frac{dw_i}{dt} = \eta y(y - \theta_M)x_i$$

$$\theta_M \sim E_\tau[y^2]$$

where x_i s the ith presynaptic input, w_i is the ith synaptic weight, and y is the postsynaptic output activity. The constant, η, refers to the learning rate and the constant, τ, is what we call the memory constant and is related to the speed of the sliding threshold. For binocular cells, the input consists of contra- and ipsilateral presynaptic inputs. For monocular cells, there are only presynaptic inputs coming from the contralateral channel. The results are extremely robust to values of τ and η, which are generally chosen for practical, rather than theoretical, considerations. Each of these constants is related to the time-step for the simulations, but given the phenomenological nature of the BCM theory, it is beyond the scope of this paper to make detailed comparisons between simulation time and real time. Furthermore, because of the fact that τ can be changed within a factor of 100 with no noticeable effect, the experiments presented here cannot be used

address the time scales of the molecular mechanisms underlying synaptic modification. All of the parameters and code for these simulations can be found on the project page for the simulation package Plasticity (http://plasticity.googlecode.com).

In the BCM learning rule, weights decrease if y is less than the modification threshold, θ_M, and increase if y is greater than the modification threshold. To stabilize learning, the modification threshold "slides" as a superlinear function of the output. The output, y, is related to the product of the inputs and the weights via a sigmoidal function, $y = \sigma(\boldsymbol{x} \cdot \boldsymbol{w})$, which places constraints on the values of the output, keeping it in the range $-1 < y < 50$. The interpretation of negative values is consistent with previous work (Blais et al. 1998), where the activity values are measured relative to spontaneous activity. Thus negative values are interpreted as activity below spontaneous. We continue this use to more easily compare with previous simulations. The role of the spontaneous level for the simulations in the natural image environment is discussed elsewhere (Blais et al. 1998).

The synaptic weights, and the modification threshold, are set to small random initial values at the beginning of a simulation. At each iteration, an input patch is generated from a combination natural images and random noise, drawn from a zero-mean uniform distribution, and presented to the neuron. The random noise is present to simulate the natural variation in responses of LGN neurons. Practically, it avoids the artificial situation of having mathematically identical inputs in the two input channels of the binocular cells. The exact values for the SD of the noise in both the open- and closed-eye cases is shown in Table 1.

After each input patch is presented, the weights are modified using the output of the neuron, the input values and the current value of the modification threshold. This process yields orientation selective cells with the natural image environment (Blais et al. 1998). We present test stimulus made from sine-gratings of 24 orientations, optimized for spatial frequency, and the response to the preferred orientation is selected as the neuron response. This is the response that is used in all of the plots. Simulations are ended when selectivity has been achieved and the responses are stable. Orientation tuning is calculated by taking the ratio of the first harmonic, F(1), of the fast Fourier transform (FFT) to the zeroeth harmonic, F(0).

Deprivation in the mouse visual system

In previous work with the BCM learning rule (Blais et al. 1999), deprivation was modeled using spatially uncorrelated noise in the deprived eye. This assumption has been shown to be necessary to be consistent with the experiments that show that presynaptic activity is needed for the ocular dominance shift in MS (Rittenhouse et al. 1999, 2006) and that more presynaptic activity in the deprived channel give rise to a faster ocular dominance shift. With BCM, the resulting ocular dominance shift in monocular deprivation occurs as a result of patterned input competing with unpatterned noise.

TABLE 1. *Default Parameters for the Simulations*

Default Parameters	
Parameter	Value
Open-eye pattern SD	1.0
Deprived eye degraded pattern SD	0.2
Deprived eye degraded pattern blur size	3 pixels
Open-eye noise SD	0.1
Deprived eye noise SD	0.1
Dark eye noise SD	0.05
Difference of Gaussian center/surround	2 pixel/6 pixel
Total simulation time	4×10^7 iterations
Memory constant, τ	1,000 iterations
Learning rate, η	5×10^{-6} iterations^{-1}

In this study, we model inputs to the deprived channel as a significantly scaled down and corrupted natural image stimulus, where the inputs are scaled down by a factor of 5 and corrupted with a Gaussian blur filter with additional random noise, again drawn from a zero-mean uniform distribution. This is to provide spatial structure to the deprived inputs in a simple and direct way, which is tunable and easy to interpret. Table 1 provides the exact parameters for the filter and the noise for deprived channels. The scaled-down factor of 5 is performed to be consistent with measurements through the lid-sutured eyes, shown in Fig. 3. Thus with the BCM learning rule and structure in the deprived channel, ocular dominance shifts in MS are a result of competition between two different qualities of patterned input: degraded versus normal patterns. BS effects are caused by selective cells presented with degraded, noisy input patterns.

RESULTS

Experimental observations of the effects of visual deprivation and recovery

To assess the effect of different deprivation protocols, we recorded VEPs (Sawtell et al. 2003) from young mice before and after the deprivation protocols. As shown previously (Frenkel and Bear 2004), 3 days of MS are sufficient to significantly reduce the magnitude of the VEP from the contralateral (C) eye, with no change in the ipsilateral (I) eye VEP (Fig. 2*A*). The C/I VEP ratio shifts significantly from ~2:1 to 1:1 ($P = 0.01$, Wilcoxon signed rank test).

The loss of deprived eye responses reflects some form of competition, as shown by a comparison of the effects of MS with a comparable period of binocular deprivation. Three days of BS causes no change in the magnitude of either the contralateral or ipsilateral eye VEP (Fig. 2*B*). Similarly, 4 days of total light deprivation by DE has no effect on VEPs (Fig. 2*D*).

If 3 days of MS are followed by 4 days BS, however, the VEP magnitudes after these 7 days are indistinguishable from the initial VEP magnitudes at the first day of recording (Fig. 2*C*). This implies that 4 days of BS produce a full recovery of VEP magnitudes from prior MS. This result is intriguing because BS alone does not seem to have any effect on peak cortical responses (Fig. 2*B*). Some clues about why recovery from deprivation can occur during BS can be found in the surprising difference between BS and DE. When MS is followed by DE (Fig. 2*E*), the ocular dominance shift is retained and is similar to the shift after MS alone.

The difference between MS followed by BS (Fig. 2*D*) and MS followed by DE (Fig. 2*E*) cannot be accounted for by our previous assumptions regarding normal and deprived rearing conditions. In particular, our previous assumptions cannot account for the recovery of the deprived eye during the 4 days of BS. We postulate that these results can be accounted for by assuming that during an MS protocol, the activity pattern in the retina is not random noise, but that some patterned vision is preserved through the sutured eyelid (Krug et al. 2001). We examined this hypothesis in the awake mouse preparation by comparing VEPs evoked through open and closed eyelids. We discovered that a VEP was clearly present when grating stimuli were presented at 0.05 cycles/degree through the closed eyelid, albeit with an amplitude diminished by ~5-fold relative to the eye-open condition (Fig. 3). We therefore explored the consequences of the assumption that deprivation causes a degraded, but not totally uncorrelated input using a model of synaptic modification in the mouse visual system.

Model of normal rearing

Our model of the mouse visual system and the training patterns appropriate for mouse simulations differ from assumption appropriate for cat simulations (see METHODS). First, the visual acuity in the mouse retina is much lower than for cat. This results in patterns of retinal activity in mouse (Fig. 1*B*) that are blurry and carry little information about the high spatial frequency features of the visual environment. Second, the mouse has a significant contralateral bias. We represent this by assuming that one half the cells in the mouse binocular region are binocular and respond equally to both eyes, whereas the other half is monocular and responds only to the contralateral eye (Fig. 1*C*).

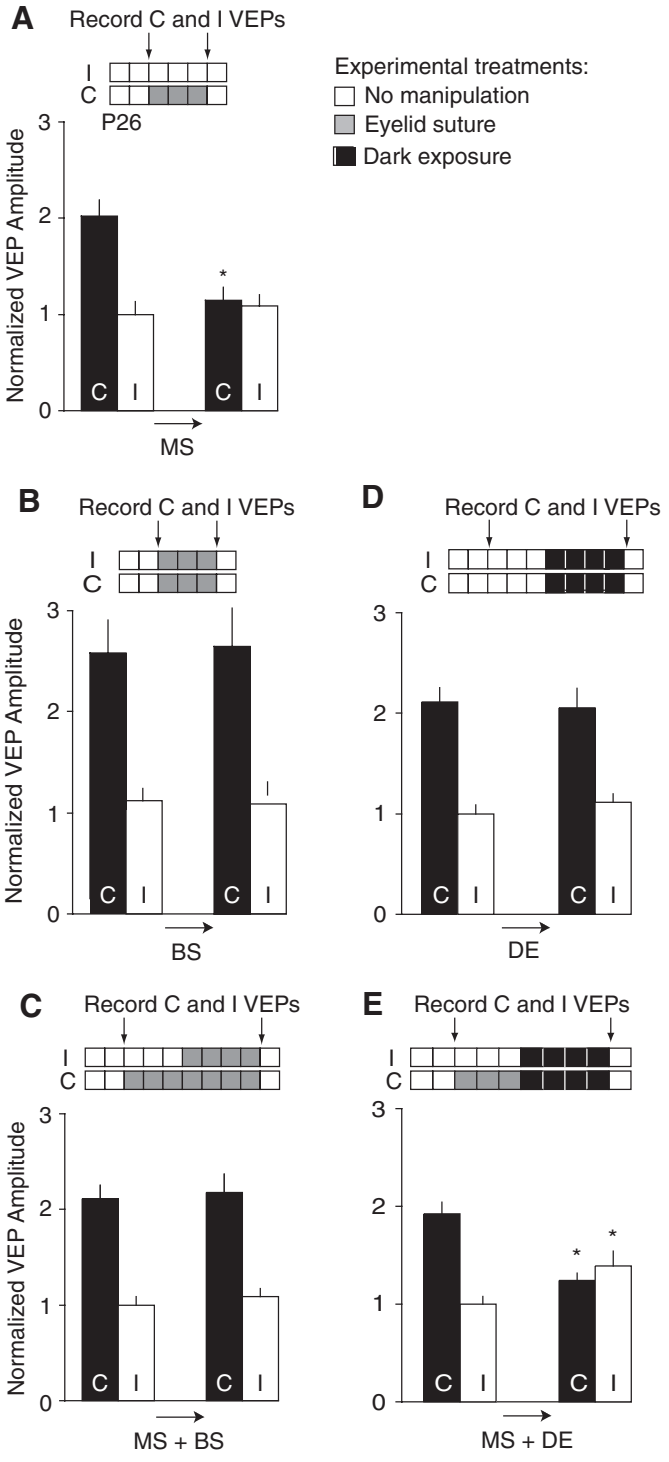

FIG. 2. Monocular deprivation and recovery: experimental results. *A*: monocular lid suture (MS) for 3 days causes depression of the contralateral visually evoked potential (VEP; $n = 8$, contralateral VEP amplitude ± SE on day 0: 217 ± 18 μV; on day 3: 123 ± 15 μV; ipsilateral amplitude on day 0: 107 ± 14 μV; on day 3: 117 ± 12 μV, $P < 0.05$ paired *t*-test). *B*: binocular lid suture (BS) for 3 days does not alter the VEPs ($n = 6$, contralateral VEP amplitude ± SE on day 0: 222 ± 31 μV; on day 3: 227 ± 35 μV; ipsilateral amplitude on day 0: 87 ± 11 μV; on day 3: 92 ± 11 μV, data previously published by Frenkel and Bear 2004). *C*: MS for 3 days followed by 4 days of BS produces responses at day 7 that are indistinguishable from responses at the beginning of the trial ($n = 5$, contralateral VEP amplitude ± SE on day 0: 156 ± 10 μV; on day 7: 161 ± 14 μV; ipsilateral amplitude on day 0: 74 ± 6 μV; on day 7: 80 ± 7 μV). *D*: 4 days of placing the animals in the dark (DE) did not change the VEPs ($n = 6$, contralateral VEP amplitude ± SE on day 0: 148 ± 31 μV; on day 7: 144 ± 32 μV; ipsilateral amplitude on day 0: 70 ± 15 μV; on day 7: 78 ± 16 μV). *E*: 4 days of DE did not affect the shift caused by 3 days of MS ($n = 10$, contralateral VEP amplitude ± SE on day 0: 144 ± 9 μV; on day 7: 92 ± 6 μV; ipsilateral amplitude on day 0: 74 ± 6 μV; on day 7: 104 ± 11 μV). *$P < 0.05$ using paired *t*-test.

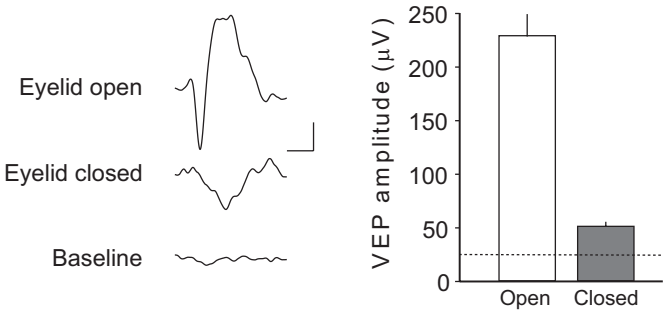

FIG. 3. VEP responses elicited through shut eyes. VEPs were recorded in response to grating stimuli (0.05 cycles per degree) at 100% contrast while both eyes were open (open bar) and following binocular deprivation by lid suture (shaded bar). Baseline recordings were made in response to a gray screen of equal luminance (dashed line). VEPs were significantly greater than baseline when both eyes were open (post hoc paired *t*-test, $P < 0.001$) and when the eyelids were sutured closed (post hoc paired *t*-test, $P < 0.001$). Post hoc statistical comparisons were done after reaching significance with repeated measures 2-way ANOVA ($P < 0.001$).

In Fig. 4, we show the development of cortical responsiveness during normal rearing (NR) (Blais et al. 1998; Law et al. 1994). NR is modeled using inputs derived from natural images, the synapses are modified with the BCM learning rule (see METHODS), and the cell develops normal orientation-selective responses. On the *left* of Fig. 4*A,* we show the maximal contralateral and ipsilateral responses to test stimuli as they develop over time in a binocular cell. The response to stimulation of both eyes is nearly identical. On the *right* of Fig. 4*A,* we show the developing responses of a monocular cell. The cortical response shown in Fig. 4*B* is a sum of the responses of the monocular and binocular cells, as would be reflected in a population measure such as a VEP, and we see that it develops the observed contralateral bias.

This is the first attempt to use images appropriate for the mouse visual system for simulations of developing cortical receptive fields. Orientation selectivity is developed with lower acuity images, but cells are more broadly tuned and are tuned to lower spatial frequency (data not shown) as would be expected for the rodent visual system (Gordon and Stryker 1996; Metin et al. 1988).

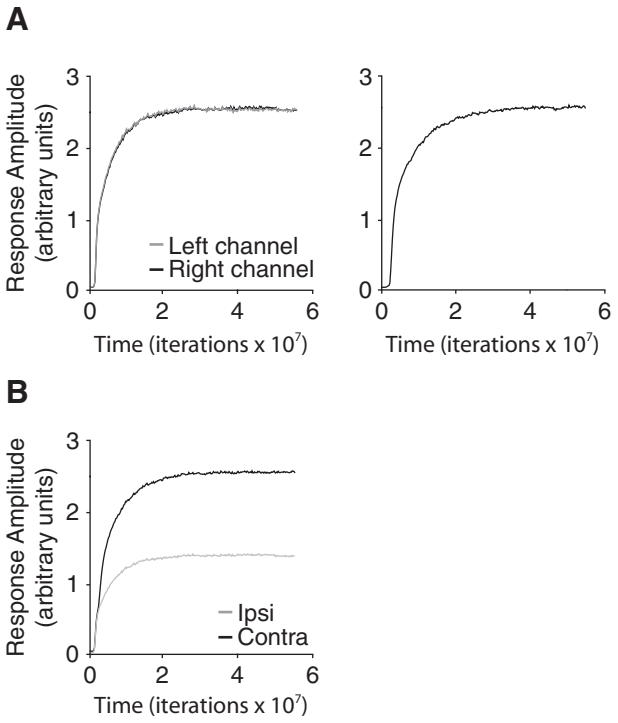

FIG. 4. Normal rearing in a mouse model. *A*: binocular (left) and monocular (right) cell responses vs. time. The y-axis represents the response of the trained neurons to test stimuli at the preferred orientation, measured in arbitrary units. As the model neuron is trained with natural images, the cell becomes selective, responding more strongly to oriented stimuli. *B*: combining the binocular and monocular responses, to mimic the VEP recordings, yields contralateral and ipsilateral responses that are used for all of the simulations. The binocular and monocular cell responses contribute equally to the contralateral responses, and the ipsilateral responses include only binocular responses from the ipsilateral channel. All responses are measured in arbitrary units. Contra-to-ipsi response ratio (C/I) is ~2:1 the for normal mouse.

Simulations of deprivation experiments and recovery

A major question posed by the experimental results of Fig. 2 is why there is such a difference between MS followed by BS and MS followed by DE. In this paper, we assume that these protocols differ in their input environment. We assume that in MS the input coming from the deprived eye is a significantly scaled-down and degraded version of the patterned input present in the nondeprived eye. Similarly, in BS, input from both eyes is degraded. We implement the degradation by convolving the inputs with a Gaussian blur filter and adding random noise (see METHODS for details). In contrast, we assume that, during DE, the activity in both channels is comprised entirely of random noise. Table 1 gives the properties of the pattern and noise in all of the deprivation protocols.

The simulated outcome of MS driven by degraded inputs (Fig. 5*A*) seems no different from the consequences deprivation resulting from uncorrelated noise. Despite the presence of structure in the retinal activity, the deprived contralateral eye is depressed, and the ratio between contra and ipsi responses (C/I) changes from 2 down to 1, as observed experimentally (Fig. 2*A*). This occurs because the open eye input has more structure than the deprived eye input and wins in the resulting competition between the two eyes. BCM theory has the property that there is competition between input patterns, with the neuron modifying its synapses to achieve maximal selectivity. As such, when the neuron is presented with an environment with two separate components, like the MS environment with degraded and nondegraded inputs, synapses will modify and the neuron will select the nondegraded inputs preferentially. Thus the results of MS can be achieved either with degraded inputs or with random noise in the deprived channel. However, as we show presently, the results of BS can be only achieved with degraded inputs.

BS following normal rearing seems to have little effect on absolute visual responsiveness (Fig. 5, *B* and *C*). However, a finer examination of the receptive fields shows us that they indeed change after BS (Fig. 6*A*)—they lose selectivity and respond to optimally to lower spatial frequencies because they become sensitive to the degraded structure in the binocularly

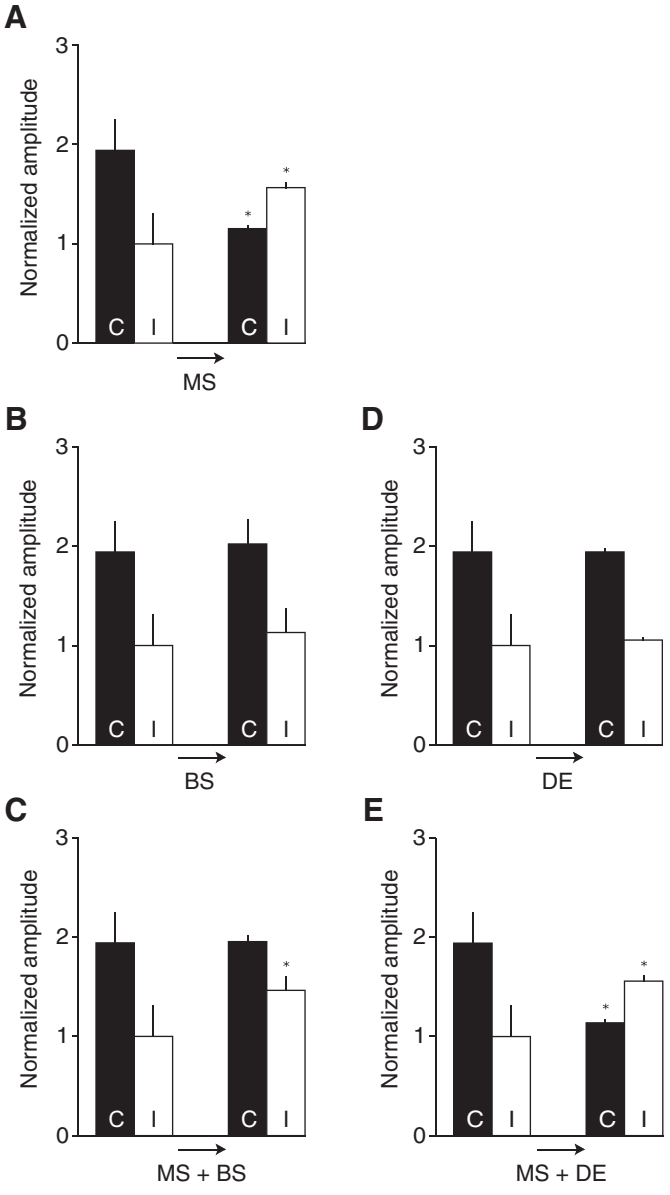

FIG. 5. Simulations of monocular deprivation and recovery. *A*: the contralateral bias is reduced during simulations of MS, in which the deprived channel is modeled as degraded and noisy patterned input. *B*: BS (2 degraded channels) does not alter the contralateral bias or absolute responsiveness. *C*: BS after MS results in a recovery of the deprived eye responses. *D*: DE does not alter the contralateral bias or absolute responsiveness. *E*: DE after MS does not result in a recovery of deprived eye responses.

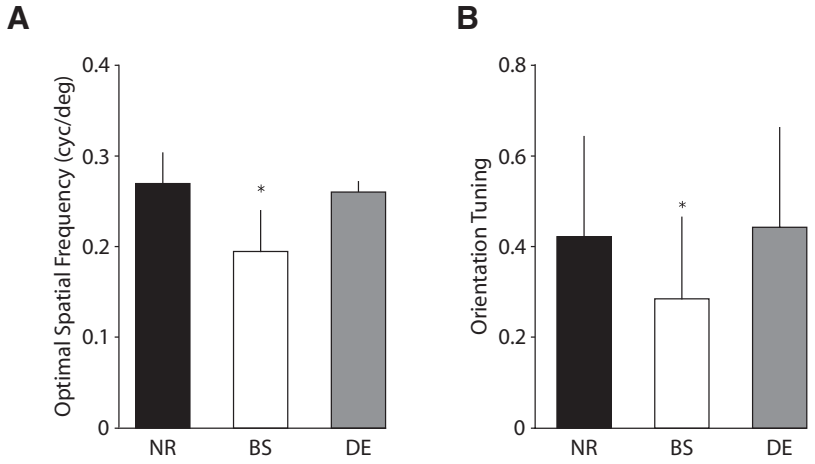

FIG. 6. Spatial frequency and orientation tuning of simulated cells after recovery. *A*: the optimal spatial frequency is reduced after BS compared with normal cells. DE results in no change in optimal spatial frequency. *B*: orientation tuning is reduced in BS and unchanged in DE compared with normal cells.

deprived channels. However, when NR is followed by DE, the receptive fields do not change appreciably—they remain selective and responsive to the same optimal spatial frequency as normal mice (Fig. 6*B*). This is one of the testable predictions of this model.

When 3 days of MS are followed by BS (Fig. 5*C*), we obtain a full recovery of the deprived eye responses. This is consistent with experimental results (Fig. 2*D*). In contrast, when MS is followed by DE, no recovery occurs (Fig. 5*E*), as observed experimentally. The recovery in the BS case occurs because the neuron retains the degraded structure in the deprived channels, in the absence of competition with a nondeprived channel. In contrast, during DE, there is no structure in the deprived input, and therefore responses cannot recover.

DISCUSSION

Previous studies showed that the BCM rule trained with an input environment composed of natural images can account for many experimental results under normal and deprived rearing conditions (Blais et al. 1999; Law et al. 1994; Shouval et al. 2002). In these previous simulations, we assumed that monocular lid suture can be represented by spatially uncorrelated random activity in the deprived channel. Here we present experimental results showing that BS results in recovery of the previously deprived eye, whereas MS followed by DE results in no recovery. These results are inconsistent with our previous assumptions. We show that we can theoretically account for these new experimental results if we change our assumptions about inputs from a channel deprived by lid suture. Here we postulate that inputs from a lid sutured channel are drastically scaled-down and degraded versions of normal mouse vision, and this assumption is sufficient to account for the new experimental observations. This new assumption can account for the new experimental results for the following reason: If the degraded input is in competition with a channel with normal vision, it will lose out and there will be depression of the response from the deprived channel. However, during BS both channels are degraded, but have sufficient visual structure for developing responsive cells, and recovering from MS. During DE, in contrast, the channels have no structure and no recovery from MS is obtained.

Structure, noise, and BCM modification

The BCM learning rule has the property that, all other things being equal, the output value is maintained when input magnitude is changed. Thus when the patterned input intensity decreases, the weights increase "homeostatically" to maintain the output. Responses to test or probe stimuli, however, will be increased relative to the responses before changing the input magnitude.

BCM has a second property that, for selective neurons, the output is inversely proportional to the number of patterns in the environment to which it is selective: neurons respond stronger to more rare patterns. One outcome of blurring is to make more patterns similar, which would make a neuron less selective and drive the weights down. Thus the more degraded the patterned input, the closer the dynamics will be to the results from previous studies (Blais et al. 1999; Law et al. 1994; Shouval et al. 2002) using only noise: ocular dominance shifts from monocular deprivation will be more pronounced, and responses will decrease for binocular deprivation.

A third property of BCM is that, if there is noise in addition to pattern, increased noise decreases the weights, again to maintain the overall mean output value. This effect is more rapid with more noise, as explored previously (Blais et al. 1999).

These three properties of the BCM modification rule put constraints on the parameter values needed to be consistent with the observed dynamics of deprivation. In the case of BS, to get no change following normal rearing and full recovery following brief MS, the noise level, amount of degradation of the input patterns, and the scale of the input patterns must be closely balanced. Thus the experiments place constraints on the parameter values. Using the parameters that are consistent with BS, the other results presented follow.

Robustness of the simulations

The results presented are robust to certain changes in the parameters or architecture and are sensitive to others. The sensitivity leads both to predictions and to a better understanding of the source of the results. Time-related parameters, such as the learning rate and the memory constant, are not critical to any of the results presented. The learning rate is chosen for the practical reason of making sure the simu-

lations run in a reasonable amount of time. The memory constant can be changed by at least a factor of 100 with no effect whatsoever; however, if it is set too high, the neuron will experience strong oscillations and never converge to a stable response.

The model includes a number of simplifying assumptions. Examples are the construction of the contra–ipsi bias and the relationship of VEP changes to the modification of postsynaptic cell activity. The exact nature and source of the contralateral bias is not well understood, so we chose a simple model until we have data to constrain the model further. Consequently, although we aim to achieve qualitative agreement, we cannot necessarily expect (and do not claim) quantitative agreement between the modeling and experimental results. For example, with the assumptions we used for the simulations, the optimal spatial frequency of simulated cortical neurons is higher than the 0.05 cycles/degree observed experimentally using VEP recordings. Achieving closer correspondence between the optimal stimuli in simulations and in vivo is possible, but computationally expensive. It would require a large increase in the receptive field size, and consequently an extremely large increase in the image dataset size, both resulting in significantly longer simulation runtime. Such quantitative changes are, however, unlikely to cause qualitative changes to the results, which arise from other assumptions.

The key assumption in this work necessary to achieve the results we present is the presence of structured input entering through the sutured eye, which we model as image degradation. The choice of image degradation, random noise in the deprived channel, and the scale of the deprived inputs are critical to these results, and they are linked. If, for example, one changes the distribution of the deprived-eye noise from a uniform distribution to a normal distribution for the noise, it would have a similar effect to increasing the magnitude of the noise. This would tend to drive a BCM neuron to lower responses in BS. To remain consistent with the observed results (i.e., no response changes in BS), one would have to use deprived-eye inputs that are either less degraded or perhaps reduced in scale.

A recent study by Mrsic-Flogel et al. (2007) used two-photon calcium imaging to measure responses of neurons after MS and BS. They observe increases in responses of binocular neurons after BS and increases in deprived-eye responses in neurons devoid of open-eye input in MS. They suggested that this finding is inconsistent with a Hebbian-type learning mechanism (BCM, specifically), and is only consistent with a general homeostatic process that preserves the net visual drive of each neuron. However, the homeostatic property of BCM, combined with the small amount of pattern present in deprived inputs, would account for the increases in deprived-eye responses they observe. On the other hand, the DE results presented here are inconsistent with the homeostatic model they propose. A homeostatic mechanism would predict even more increases in responses following DE compared with BS, which is not observed. BCM correctly predicts no change in responses following DE.

Origin of structured input

In these simulations, we assumed that a channel deprived by lid suture carries a diminished and degraded version of the patterned input and that dark rearing leads to uncorrelated noise. It is clear from the difference between the experiments in which monocular deprivation is followed by BS or DE that lid suture deprivation is very different from light removal. The critical difference may be that enough light can enter through the sutured eyelid to evoke cortical responses, albeit weakly (Fig. 3). Of course, the "patterns" resulting from the light through the eyelid are certainly not equivalent to patterned input during normal vision. It is possible that the light intensity through the sutured lid generates activity that yields structure (correlations) either in the retina or the LGN. Another possibility is the recruitment of feedback from the cortex to LGN, which could influence the correlations in LGN neuronal firing, which could lead to correlated input back to the cortex. Each of these possibilities is testable and should help us determine the critical properties of the visual system involved.

Future directions

A more biophysical model may be necessary to get the detailed dynamics, but the simulations presented here already help us to determine the issues at hand. Some of the assumptions need to be explored both theoretically and experimentally. For example, the origin of the contralateral bias is not completely understood and might play a significant role in the dynamics of deprivation, although the results presented here are robust to different models of the bias. Most importantly, it is a prediction of this model that the LGN activity during lid suture is more correlated than the activity during dark exposure. These correlations should be experimentally verifiable, and their source explored.

The mouse visual cortex has now become the standard model to study ocular dominance plasticity. Among numerous advantages, the absence ocular dominance columns and other types of cortical anisotropy make chronic recordings of response changes in awake animals feasible, yielding data on changes in absolute and relative visual responsiveness when visual experience is manipulated. Moreover, VEP recordings can be made from layer 4, where information from the two eyes first converges onto the same neurons. The relative simplicity of the mouse visual cortex and the ability to measure the dynamics of plasticity at thalamocortical synapses make this an excellent system to bring theoretical models into closer correspondence with biological reality.

GRANTS

This work was partially supported by Collaborative Research in Computational Neuroscience Grant NSF 0515285 from the National Science Foundation and the National Eye Institute.

REFERENCES

Bienenstock EL, Cooper LN, Munro PW. Theory for the development of neuron selectivity: orientation specificity and binocular interaction in visual cortex. *J Neurosci* 2: 32–48, 1982.

Blais BS, Intrator N, Shouval HZ, Cooper LN. Receptive field formation in natural scene environments. Comparison of single-cell learning rules. *Neural Comput* 10: 1797–1813, 1998.

Blais BS, Shouval HZ, Cooper LN. The role of presynaptic activity in monocular deprivation: comparison of homosynaptic and heterosynaptic mechanisms. *Proc Natl Acad Sci USA* 96: 1083–1087, 1999.

Blakemore C. The conditions required for the maintenance of binocularity in the kitten's visual cortex. *J Physiol* 261: 423–444, 1976.

Drager UC, Olsen JF. Origins of crossed and uncrossed retinal projections in pigmented and albino mice. *J Comp Neurol* 191: 383–412, 1980.

Frenkel MY, Bear MF. How monocular deprivation shifts ocular dominance in visual cortex of young mice. *Neuron* 44: 917–923, 2004.

Frenkel MY, Sawtell NB, Diogo AC, Yoon B, Neve RL, Bear MF. Instructive effect of visual experience in mouse visual cortex. *Neuron* 51: 339–349, 2006.

Gordon JA, Stryker MP. Experience-dependent plasticity of binocular responses in the primary visual cortex of the mouse. *J Neurosci* 16: 3274–3286, 1996.

Grubb MS, Thompson ID. Quantitative characterization of visual response properties in the mouse dorsal lateral geniculate nucleus. *J Neurophysiol* 90: 3594–3607, 2003.

Jeon CJ, Strettoi E, Masland RH. The major cell populations of the mouse retina. *J Neurosci* 18: 8936–8946, 1998.

Krug K, Akerman CJ, Thompson ID. Responses of neurons in neonatal cortex and thalamus to patterned visual stimulation through the naturally closed lids. *J Neurophysiol* 85: 1436–1443, 2001.

Law CC, Bear MF, Cooper LN. Role of the visual environment in the formation of receptive fields according to the BCM theory. *Prog Brain Res* 102: 287–301, 1994.

Metin C, Godement P, Imbert M. The primary visual cortex in the mouse: receptive field properties and functional organization. *Exp Brain Res* 69: 594–612, 1988.

Mrsic-Flogel TD, Hofer SB, Ohki K, Reid RC, Bonhoeffer T, Hubener M. Homeostatic regulation of eye-specific responses in visual cortex during ocular dominance plasticity. *Neuron* 54: 961–972, 2007.

Rittenhouse CD, Shouval HZ, Paradiso MA, Bear MF. Monocular deprivation induces homosynaptic long-term depression in visual cortex. *Nature* 397: 347–350, 1999.

Rittenhouse CD, Siegler BA, Voelker CC, Shouval HZ, Paradiso MA, Bear MF. Stimulus for rapid ocular dominance plasticity in visual cortex. *J Neurophysiol* 95: 2947–2950, 2006.

Sawtell NB, Frenkel MY, Philpot BD, Nakazawa K, Tonegawa S, Bear MF. NMDA receptor-dependent ocular dominance plasticity in adult visual cortex. *Neuron* 38: 977–985, 2003.

Shouval HZ, Castellani GC, Blais BS, Yeung LC, Cooper LN. Converging evidence for a simplified biophysical model of synaptic plasticity. *Biol Cybern* 87: 383–391, 2002.

Sterling P, Freed MA, Smith RG. Architecture of rod and cone circuits to the on-beta ganglion cell. *J Neurosci* 8: 623–642, 1988.

Stone C, Pinto LH. Response properties of ganglion cells in the isolated mouse retina. *Vis Neurosci* 10: 31–39, 1993.

Wiesel TN, Hubel DH. Single-cell responses in striate cortex of kittens deprived of vision in one eye. *J Neurophysiol* 26: 1003–1017, 1963.